Asian Journal of Chemistry; Vol. 23, No. 6 (2011), 2762-2766

ASIAN JOURNAL OF CHEMISTRY

www.asianjournalofchemistry.co.in

Destruction Mechanism and Kinetic of Formaldehyde by O_3 and OH Radicals

ZHENGCHENG WEN[1,*], JIANGRONG XU[1], ZHIHUA WANG[2], JUNHU ZHOU[2] and KEFA CEN[2]

[1]College of Science, Hangzhou Dianzi University, Hangzhou 310018, P.R. China
[2]State Key Laboratory of Clean Energy Utilization (Zhejiang University), Hangzhou 310027, P.R. China

*Corresponding author: Fax: +86 571 87951616; Tel: +86 571 87953162; E-mail: wenzc@hdu.edu.cn

(*Received*: 22 October 2010; *Accepted*: 28 February 2011) AJC-9658

The catalytic oxidation technology has been believed as the most promising technology of formaldehyde destruction because of its high efficiency, thorough destruction and easy application. For the catalytic oxidation technology, formaldehyde was radically destructed by the O_3 and OH radicals, which were produced by various catalytic ways such as photo-catalysis and electro-catalysis. Due to its fundamental importance, the destruction mechanism of formaldehyde by O_3 and OH radicals was investigated in detail by employing quantum chemical calculation in this work. The microcosmic reaction process was calculated and discussed in detail by the UB3LYP/6-31G(d) method and the activation energies were calculated by the QCISD(T)/6-311g(d,p) method. Furthermore, the kinetic parameters were also calculated by the transition state theory. Theoretical results showed that the activation energies of the HCHO + OH reaction (3.57 kcal/mol) was much lower than that of the HCHO + O_3 (20.20 kcal/mol) and the rate constant of the HCHO + OH reaction was much larger than that of the HCHO + O_3 reaction. This indicated that the OH radical has much stronger ability to destruct formaldehyde than the O_3 radical, which was in conformity with that the OH radical has much stronger oxidation character than the O_3 radical. Moreover, by comparing, the theoretical results were in agreement with the experimental results in literature, which indicated the theoretical calculation in this work was reasonable and reliable.

Key Words: Formaldehyde, O_3, OH, Destruction mechanism, Quantum chemistry.

INTRODUCTION

At present, the pollution of indoor air has considerably been taken attention abroad as an important environmental problem. As a ubiquitous pollutant in the indoor air, formaldehyde has great adverse effects on human health and is considered to cause cancer and abnormality by WHO[1,2]. Great efforts have been made for economical and effective destruction of formaldehyde. Nowadays, the catalytic oxidation technology has been considered as the most promising technology of formaldehyde destruction because of its high efficiency, thorough destruction and easy application[3-11].

According to different catalytic ways, the catalytic oxidation technology can be classified into three kinds: (1) photo-catalysis[3,4]: strong oxidants such as O_3 and OH radicals are produced *via* photo-chemical reaction by making use of sunlight in the near-UV irradiation and then the O_3 and OH radicals destruct formaldehyde effectively; (2) electro-catalysis[5,6]: strong oxidants such as O_3 and OH radicals are produced *via* plasma chemical reaction by various techniques of plasma discharge; (3) semiconductor metal oxides catalysis[7-9]: in virtue of many activity photo-holes, TiO_2, MnO_2 and other semiconductor metal oxide adsorb H_2O and O_2 on their surface and convert them into O_3 and OH radicals to achieve the aim of destructing formaldehyde effectively. The efficiency of electro-catalytic destruction of formaldehyde up to 80 %[5,6], but the efficiency destruction of formaldehyde of only using semiconductor metal oxide catalysis or photo-catalysis is quite low. Therefore, these two catalytic ways are always used together to improve the destruction efficiency. UV/TiO_2 technology is its typical technology[9,10]. The other way to increase the destruction efficiency is adding the generated ozone[11,12]. On the one hand, it can increase O_3 content. On the other hand, the added O_3 can react with H_2O to yield the OH radical *via* semiconductor metal oxide catalysis or photo-catalysis. Both the increasing of O_3 content and enhancing the formation of OH can significantly improve the destruction efficiency of formaldehyde.

As noted above, the catalytic oxidation technology is that O_3 and OH radicals are produced by various ways of catalysis in order to destruct formaldehyde effectively. As shown in Table-1, O_3 and OH radicals are the strongest natural oxidants after fluorine. They can destruct formaldehyde unreservedly. To promote the further development of catalytic oxidation

TABLE-1
ELECTRODE POTENTIALS OF NATURE OXIDANTS

Name	Formula	Standard electrode potentials (V)
Fluorine	F_2	2.87
Hydroxide radical	OH	2.80
Ozone	O_3	2.07
Hydrogen peroxide	H_2O_2	1.78
Potassium permanganate	$KMnO_4$	1.67
Chloride dioxide	ClO_2	1.50
Chlorine	Cl_2	1.36
Oxygen	O_2	1.23

technology, basic investigation on the destruction mechanism of formaldehyde by O_3 and OH radicals is essential. With the development of modern physical chemistry theory and modern computer technology, quantum chemical calculation has become an important method for investigating chemical reactions. Thus the destruction mechanism of formaldehyde by O_3 and OH radicals was investigated by employing quantum chemical calculation. For simplicity, the following reactions were calculated and analyzed in detail to investigate the destruction mechanism of formaldehyde by O_3 and OH radicals.

$$HCHO + O_3 \longrightarrow Products$$

$$HCHO + OH \longrightarrow Products$$

CALCULATION DETAILS

Quantum chemical calculations in present studies were carried out using the Gaussian 2003 suite of programs[13]. All geometries of the reactants, products and stationary points were fully optimized by the unrestricted B3LYP method using the 6-31G(d) basis set[14,15]. The character of all stationary points was confirmed by a frequency calculation at the same level. If no imaginary frequency is shown, the stationary point was confirmed as intermediate. And if only one imaginary frequency is obtained, the stationary point was confirmed as transition state. The energies of stationary points were calculated by the QCISD(T)/6-311g(d,p) method[16,17] based on the geometry optimizations of the UB3LYP/6-31G(d) method. After corrected with zero-point energies (E_{ZPE}), the relative energies of stationary points along the reaction processes and the activation energy (ΔE) were calculated. Owing to average overestimation of the UB3LYP/6-31g(d) method[18], the raw calculated values of E_{ZPE} were scaled by 0.9613. For all the calculations, the spin contaminations were carefully checked and no significant spin contamination was found, which indicates that the quantum chemical calculations in this paper are reliable.

Based on the mechanism study, the reaction rate constant was calculated by the transition state theory (TST). The involved equations[19,20] are given below.

$$k(T) = \lambda\left(\frac{k_B T}{h}\right)\left(\frac{Q^{\neq}}{Q_A Q_B}\right)\exp\left(-\frac{E_a}{RT}\right)$$

$$\lambda = 1 + \frac{1}{24}\left(\frac{h\nu^{\neq}}{k_B T}\right)^2$$

Here, λ = correct factor for the quantum effect, k_B = Boltzman constant, T = temperature, h = Planck constant, $\nu^{\neq}$ = imaginary vibrational frequency of transition state, E_a = activation energy, $Q^{\neq}$ and Q_A/Q_B are the total partial functions of the transition state and reactant, respectively.

RESULTS AND DISCUSSION

Reaction processes: For the HCHO + O_3 and HCHO + OH reactions, the geometry optimizations of stationary points such as reactants, products, intermediates (M) and transition states (TS) along reaction processes were performed by UB3LYP/6-31g(d) method. Based on the analysis of each stationary point, the microcosmic reaction processes were depicted in Figs. 1, 2 and 5.

As shown in Figs. 1 and 2, the reaction process of HCHO + O_3 can be divided as two steps, which were discussed as follows.

Section-I: The cleavage of HCHO was not only the first step but also the key step during the overall reaction. The cleavage of HCHO stands for the destruction of HCHO. The attacking of ozone to formaldehyde occurs on one of the H atoms. For the attacking, two mechanistically different routes were found: the terminal oxygen atom of ozone (O7) and the oxygen atom of HCHO (O2) are either on the different side (*trans*-route) or on the same side of the O6-O5-H4-C1 ring (cis-route). The reaction processes of these two different routes are similar to each other. For each route, HCHO are attacked by O_3 to form the intermediates (HCO and HO3) *via* transition state directly. During the process of the *trans*-routes, the distance between O5 atom of O_3 and H4 atom of HCHO reduces gradually (∞ Å $\rightarrow$ 2.082 Å $\rightarrow$ 1.425 Å, ∞ denotes the distance exceeding the range of bond forming, as the same in the following text), which indicates the formation of O5-H4 bond and the distance between H4 atom and C1 atom of HCHO increases gradually (1.206 Å $\rightarrow$ 1.328 Å $\rightarrow$ ∞ Å), which indicates the breaking of H4-C1 bond. The similar changes of geometric configurations can also be found during the process of the *cis*-route. All the changes of geometric configurations on the reactants, transition states and intermediates can describe the reaction process clearly.

Section-II: The cleavage of the intermediate HO3 was the second step of the overall reaction. As shown in Fig. 2, HO3 are destructed to form the products (O2 and OH) through the transition state. During the reaction process, the distance between O5 atom and O6 atom increases gradually (1.503 Å $\rightarrow$ 1.871 Å $\rightarrow$ ∞ Å). The changes of bond distance indicated the formation of O5-O6 bond.

Based on geometry optimizations made by UB3LYP/6-31G(d) method, all potential energies of stationary points along the HCHO + O_3 $\rightarrow$ products reaction were calculated by QCISD(T)/6-311g(d,p) method. After corrected with ZPE, the energies variation in reaction processes of the HCHO + O_3 $\rightarrow$ products reaction were illustrated in Figs. 3 and 4. According to transition state theory (TST), the activation energies of the correlative reactions were calculated. The calculated activation energies in the section I and II of the HCHO + O_3 $\rightarrow$ products reaction were 21.20/20.20 kcal/mol and 1.45 kcal/mol, respectively. By comparing, the section I can be considered as the

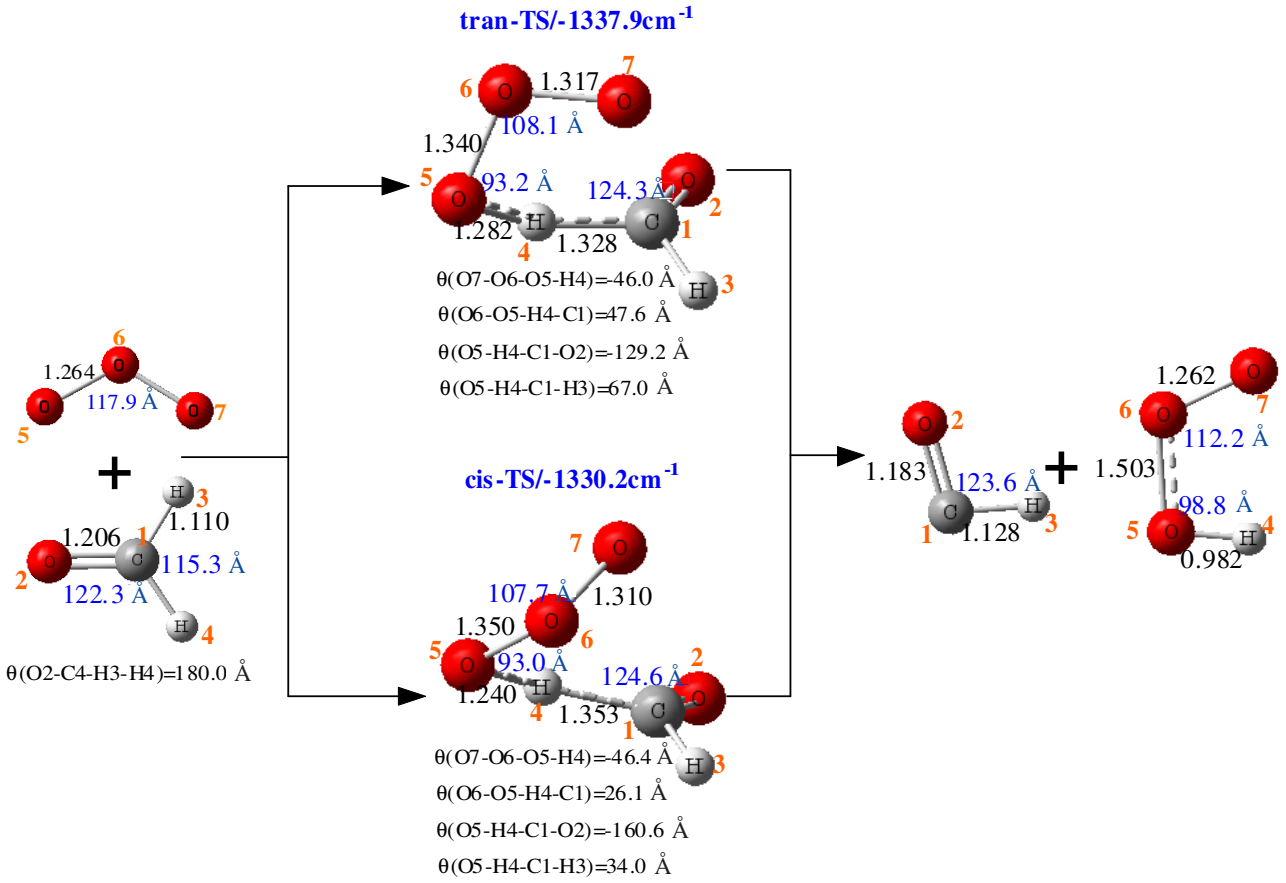

Fig. 1. Optimized geometries of the stationary points along the HCHO + O_3 reaction: section-I. Angles are given in degrees and bond distances are given in angstroms

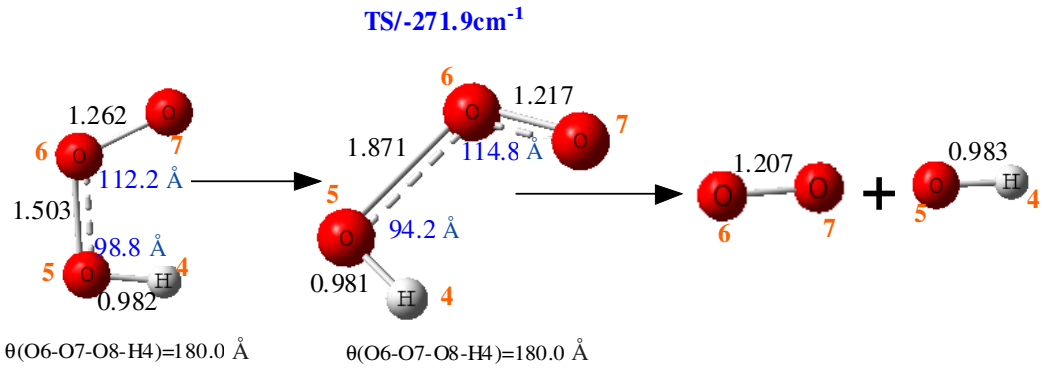

Fig. 2. Optimized geometries of the stationary points along the HCHO + O_3 reaction: section-II. Angles are given in degrees and bond distances are given in angstroms

rate-determining step for the overall reaction. As shown in Fig. 3, for section I, the calculated activation energies in the *trans*-route and *cis*-route were 21.20 and 20.20 kcal/mol, respectively. Since the reaction always process along the path with lower activation energy. The *trans*-route in section I can be believed as the rate-determining step for the overall reaction.

For the HCHO + OH reaction, the reaction process began with the attacking of the O atom of OH to the H atom of HCHO. As shown in Fig. 5, the intermediate was formed *via* transition state and then, the intermediate break to form smaller molecules (H_2O and HCO). During the process of the HCHO + OH reaction, the distance between O5 atom of OH and H4 atom of HCHO reduces gradually (∞ Å → 1.607 Å → 1.040 Å → 0.969 Å), which indicates the formation of O5-H4 bond and the distance between H4 atom and C1 atom of HCHO increases gradually (1.110 Å → 1.161 Å → 1.622Å → ∞ Å), which indicates the breaking of H4-C1 bond. The changes of geometric configurations of the reactants, transition states and intermediates can describe the reaction process clearly.

As well as the HCHO + O_3 reaction, the energies variation along the reaction process of the HCHO + OH reaction were obtained by the QCISD(T)/6-311g(d,p)//UB3LYP/6-31G (d) method and illustrated in Fig. 6. Since the energy of the intermediate was lower than that of the reactant, the intermediate can be believed to be quite stable. Therefore, the formation of

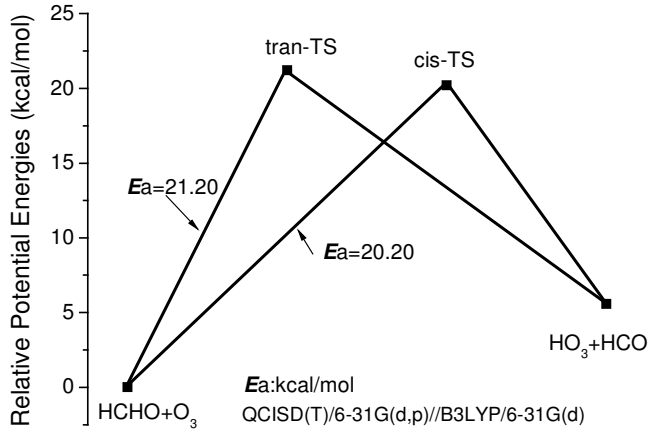

Fig. 3. Relative energies of stationary points along the HCHO + O_3 reaction: section-I

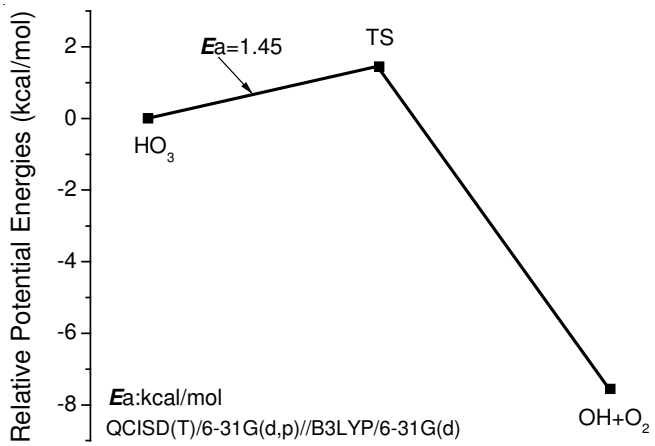

Fig. 4. Relative energies of stationary points along the HCHO + O_3 reaction: section-II

the intermediate turned out to be the rate-determining step and the calculated activation energy of the overall reaction was 3.57 kcal/mol.

Kinetic study: The calculated activation energies of the HCHO + O_3 and HCHO + OH reaction were 20.20 and 3.57 kcal/mol, respectively. Based on the calculation and analysis above, the rate constant of these two reactions were calculated by the transition state theory (TST) and the results were illustrated in Figs. 7 and 8. Moreover, the Arrhenius expressions and the reaction rates at 298 K were also obtained and compared with the experimental results were shown in Table-2.

TABLE-2
KINETIC PARAMETERS OF THE HCHO + O_3 AND HCHO + OH REACTIONS (k: $cm^3\ mol^{-1}\ s^{-1}$)

Reaction	HCHO + OH → products	HCHO + O_3 → products
Arrhenius expression (TST)	2.60×10^{15} exp (-18267/RT)	4.53×10^{12} exp (-84766/RT)
Arrhenius expression (exp.)[199]	3.89×10^{13} exp (-5857/RT)	–
k^{298} (TST)	1.66×10^{12}	6.36×10^{-3}
k^{298} (exp.)	3.68×10^{12} [Ref. 21]	1.26×10^{0} [Ref. 22]

For the HCHO + OH reaction, the calculated reaction rate constant was a little larger than the experimental result at lower temperature and a little lower than the experimental result at higher temperature, which can be seen in Fig. 7. Considering the system error of theoretical calculation, the rough agreement between the calculated results and the experimental results is tolerable. For the HCHO + O_3 reaction, the Arrhenius expression was unfortunately not found in literature to compare with the theoretical results and only the reaction rate constant at 298 K was found. By comparing, the calculated reaction rate constant at 298 K was in rough agreement with the experimental result[21], which can be seen in Table-2. The rough agreement between the calculated results and the experimental results both for the CHO + O_3 reaction and for CHO + OH reaction indicated that the mechanism and kinetic study by employing quantum chemical calculation was reasonable and reliable.

By comparing (Figs. 7 and 8), it can be found that the calculated rate constant of the HCHO + OH reaction was much larger than that of the HCHO + O_3 reaction, which was in conformity with the activation energies of the HCHO + OH reaction (3.57 kcal/mol) and much lower than that of the HCHO + O_3 (20.20 kcal/mol). This finding was in good agreement with the experimental result. Since the rate constant of the HCHO + OH reaction is much larger than that of the HCHO + O_3 reaction, it can be believed that the OH radical has much stronger ability to degrade formaldehyde than the O_3 radical. This may be explained by suggesting that the OH radical has much stronger oxidation character than the O_3 radical (Table-1).

Conclusion

The destruction mechanism of formaldehyde by O_3 and OH radicals was investigated by employing quantum chemical calculation. The microcosmic reaction process was calculated and discussed by the UB3LYP/6-31G(d) method and the activation energies were calculated by the QCISD(T)/6-311g(d,p)

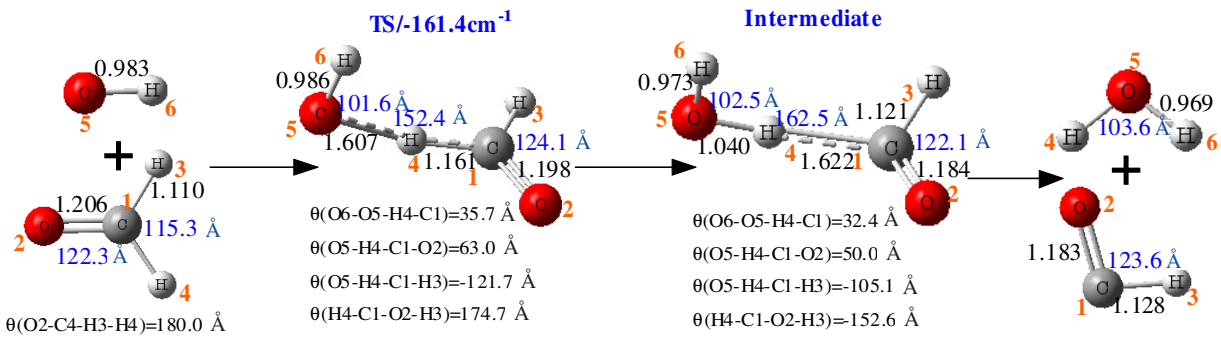

Fig. 5. Optimized geometries of the stationary points along the HCHO + OH reaction. Angles are given in degrees and bond distances are given in angstroms

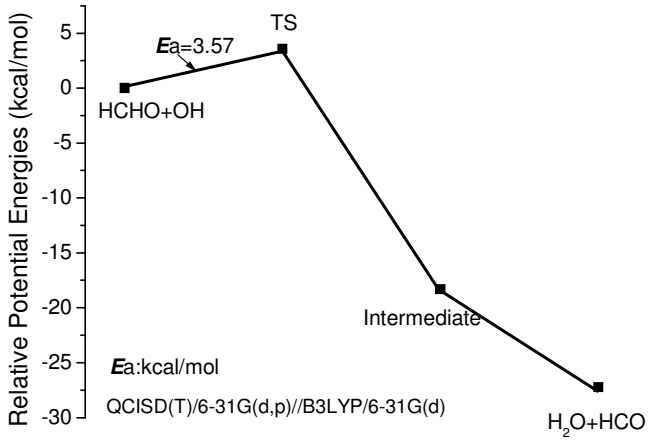

Fig. 6. Relative energies of stationary points along the HCHO + O_3 reaction

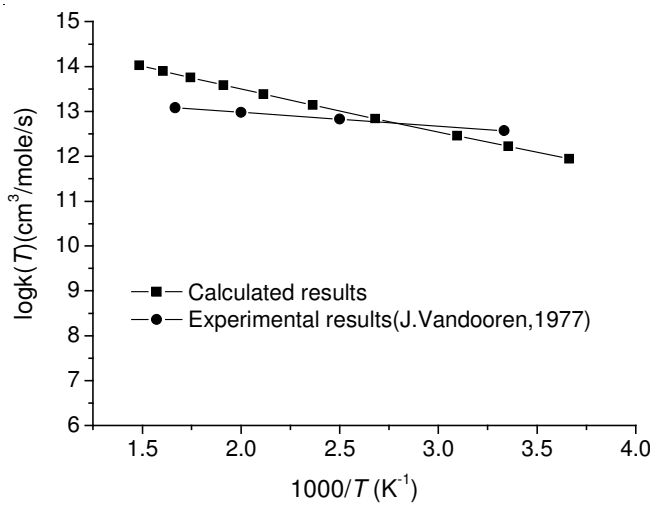

Fig. 7. Rate constant k calculated from TST: the HCOH + OH reaction

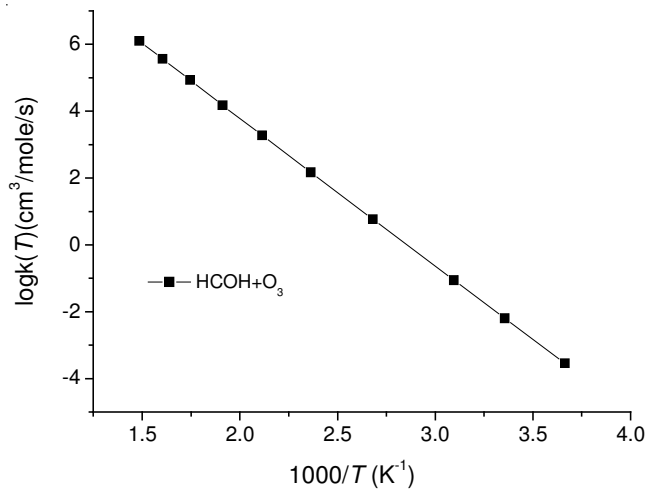

Fig. 8. Rate constant k calculated from TST: the HCOH + O_3 reaction

method. Furthermore, the kinetic parameters were also calculated by the transition state theory. Theoretical results showed that the activation energies of the HCHO + OH reaction (3.57 kcal/mol) was much lower than that of the HCHO + O_3 (20.20 kcal/mol) and the rate constant of the HCHO + OH reaction was much larger than that of the HCHO + O_3 reaction. This indicated that the OH radical has much stronger ability to destruct formaldehyde than the O_3 radical, which was in conformity with that the OH radical has much stronger oxidation character than the O_3 radical. And so, by comparison with the O_3 radical, the OH radical should be considered in the further investigation on the catalytic oxidation technology. It can be believed that the theoretical results in this paper will supply useful theory basis for further investigation on the destruction of the formaldehyde by the catalytic oxidation technology.

ACKNOWLEDGEMENTS

The authors acknowledged the financial support of the Key Project of the National Natural Science Foundation of China (Grand No. 51006030).

REFERENCES

1. L. Zhang, C. Steinmaus, D.A. Eastmond, X.K. Xin and M.T. Smith, *Mut. Res*., **681**, 150 (2009).
2. X. Tang, Y. Bai, A. Duong, M.T. Smith, L. Li and L. Zhang, *Environ. Int.*, **35**, 1210 (2009).
3. W.H. Ching, M. Leung, D.Y. C. Leung, *Solar Energy*, **77**, 129 (2004).
4. F. Shiraishi and S. Yamagucui, *Chem. Eng. Sci*., **58**, 927 (2003).
5. D.G. Storch and M.J. Kushner, *J. Appl. Phys*., **73**, 51 (1993).
6. M.B. Chang and C.C. Lee, *Environ. Sci. Tech*., **29**, 181 (1995).
7. E. Sahle-Demessie and V.G. Devulapelli, *Appl. Catal. B: Environ*., **84**, 408 (2008).
8. D.L. Liao, X.Y. Xiao, Q. Deng, H.P. Zhang and C.X. Wan, *Envion. Protect. Chem. Ind*., **23**, 191 (2003).
9. H. Ichiura, T. Kitaoka and H. Tanaka, *Chemosphere*, **50**, 79 (2003).
10. L. Yang, Z. Liu, J. Shi, Y. Zhang, H. Hu and W. Shangguan, *Sep. Purif. Technol*., **54**, 204 (2007).
11. Y.-S. Shen and Y. Ku, *Chemosphere*, **38**, 1855 (1999).
12. H. Qi, D.-Z. Sun and G.-Q. Chi, *J. Environ. Sci*., **19**, 1136 (2007).
13. M.J. Frisch, G.W. Trucks, H.B. Schlegel, G.E. Scuseria, M.A. Rob, J.R. Cheeseman, J.A. Montgomery Jr., T. Vreven, K.N. Kudin, J.C. Burant, J.M. Millam, S.S. Iyengar, J. Tomasi, V. Barone, B. Mennucci, M. Cossi, G. Scalmani, N. Rega, G.A. Petersson, H. Nakatsuji, M. Hada, M. Ehara, K. Toyota, R. Fukuda, J. Hasegawa, M. Ishida, T. Nakajima, Y. Honda, O. Kitao, H. Nakai, M. Klene, X. Li, J.E. Knox, H.P. Hratchian, J.B. Cross, V. Bakken, C. Adamo, J. Jaramillo, R. Gomperts, R.E. Stratmann, O. Yazyev, A.J. Austin, R. Cammi, C. Pomelli, J.W. Ochterski, P.Y. Ayala, K. Morokuma, G.A. Voth, P. Salvador, J.J. Dannenberg, V.G. Zakrzewski, S. Dapprich, A.D. Daniels, M.C. Strain, O. Farkas, D.K. Malick, A.D. Rabuck, K. Raghavachari, J.B. Foresman, J.V. Ortiz, Q. Cui, A.G. Baboul, S. Clifford, J. Cioslowski, B.B. Stefanov, G. Liu, A. Liashenko, P. Piskorz, I. Komaromi, R.L. Martin, D.J. Fox, T. Keith, M.A. Al-Laham, C.Y. Peng, A. Nanayakkara, M. Challacombe, P.M.W. Gill, B. Johnson, W. Chen, M.W. Wong, C. Gonzalez and J.A. Pople, Gaussian 03 (Gaussian, Inc., Wallingford, CT) (2003).
14. C. Lee, W. Yang and R.G. Parr, *Phys. Rev. B*, **37**, 785 (1988).
15. A.D. Becke, *J. Chem. Phys*., **98**, 5648 (1993).
16. J. Gauss and C. Cremer, *Chem. Phys. Lett*., **150**, 280 (1988).
17. E.A. Salter, G.W. Trucks and R.J. Bartlett, *J. Chem. Phys*., **90**, 1752 (1989).
18. A.P. Scott and L. Random, *J. Phys. Chem*., **100**, 16502 (1996).
19. M. Dupuis, G. Fitzgerald, B. Hammond and W.A. Lester, *J. Chem. Phys*., **84**, 2691 (1986).
20. D. Hwang and A.M. Mebel, *J. Chem. Phys*., **109**, 10847 (1998).
21. V. Vasudevan, D.F. Davidson and R.K. Hanson, *Int. J. Chem. Kinet*., **37**, 98 (2005).
22. S. Braslavsky and J. Heicklen, *Int. J. Chem. Kinet*., **8**, 801 (1976).